Superlattices and Microstructures 81 (2015) 88–96

Contents lists available at ScienceDirect

Superlattices and Microstructures

journal homepage: www.elsevier.com/locate/superlattices

The photovoltaic performance of CdS quantum dots sensitized solar cell using graphene/TiO_2 working electrode

Ali Badawi [a,*], N. Al-Hosiny [a,b], S. Abdallah [c]

[a] Department of Physics, Faculty of Science, Taif University, Taif, Saudi Arabia
[b] Department of Physics, Faculty of Science, Aljouf University, Aljouf, Saudi Arabia
[c] Department of Mathematical and Physical Engineering, Faculty of Engineering (Shoubra), Benha University, Cairo, Egypt

ARTICLE INFO

Article history:
Received 5 October 2014
Received in revised form 20 December 2014
Accepted 10 January 2015
Available online 7 February 2015

Keywords:
Graphene
Nanocomposite photoanode
Back recombination rate
Quantum dots sensitized solar cell
SILAR

ABSTRACT

Graphene/titania (G/TiO_2) nanocomposite photoanodes were fabricated for CdS quantum dots sensitized solar cells (QDSSCs) applications. The effect of G/TiO_2 ratio (0, 0.1, 0.2, 0.5, and 1.0 wt.%) on the photovoltaic performance of CdS QDSSCs was investigated. CdS QDs were deposited onto G/TiO_2 nanocomposite films by successive ionic layer adsorption and reaction (SILAR) technique for six cycles. The current density–voltage (J–V) characteristic curves of the assembled solar cells were measured at AM1.5 simulated sunlight. The optimal G/TiO_2 ratio was 0.2 wt.% for photovoltaic performance. CdS QDSSCs based on 0.2 wt.% G/TiO_2 nanocomposite photoanode achieve 32% increase in conversion efficiency (η) compared with those based on plain TiO_2 NPs photoanode. The photovoltage–decay curves of the assembled cell were recorded. The electron–hole back recombination rates decrease significantly for CdS QDSSCs based on 0.2 wt.% ratio of G/TiO_2 nanocomposite photoanode. The lifetime constants (τ) is much larger for CdS QDSSCs based on 0.2 wt.% ratio of G/TiO_2 nanocomposite photoanode compared to those based on plain TiO_2 NPs photoanodes.

© 2015 Elsevier Ltd. All rights reserved.

* Corresponding author. Tel.: +966 543414808; fax: +966 27241880.
E-mail address: adaraghmeh@yahoo.com (A. Badawi).

http://dx.doi.org/10.1016/j.spmi.2015.01.024
0749-6036/© 2015 Elsevier Ltd. All rights reserved.

1. Introduction

Currently, quantum dots (QDs) have attracted significant attention due to their unique electronic and optical properties, large intrinsic dipole moments, and intrinsically stronger light absorbers [1,2]. The ability of tuning QDs band gaps to match the sunlight spectra makes them attractive candidates as sensitizers in solar cells applications [1,3,4]. Quantum dots sensitized solar cells (QDSSCs) are very promising third-generation solar cells. QDSSCs will grant a technically and economically credible alternative to conventional solar cells; silicon photovoltaics or dye-sensitized solar cells (DSSCs) [1]. The latter cells have many limitations, such as organic dyes contaminate environment by the release of the toxic and water pollution [5]. A perfect QDSSC, just like DSSC, contains QDs sensitized a wide band gap semiconductor film electrode, a redox electrolyte, and a counter electrode [6,7]. The wide band gap semiconductor such as TiO_2 nanoparticles (NPs) and ZnO NPs plays a significant role in the transportation of generated electrons and back recombination rates [1]. Several research efforts have already been carried out to enhance the photovoltaic performance of solar cells [8–10] either by increasing the solar light absorption range or minimizing the electron–hole recombination rates [5,11].

Many studies were carried out using semiconductor QDs as photosensitizers: CdS [12], CdSe [13], CdTe [1], PbSe [14], PbS [15], InAs [16]. Cadmium chalcogenides (CdX; X = S, Se, and Te) QDs are relatively simple to synthesize, and easy to control their size in order to harvest as much light energy in the visible region of the solar spectrum as possible. Many techniques are used to adsorb QDs onto large band gap semiconductor oxides. A well-known technique called successive ionic layer adsorption and reaction (SILAR) [4] is used in this study. SILAR method provides a good surface coverage and produces a high-quality nanoparticles in a large scale [17].

Lately, graphene, the two-dimensional carbon nanomaterial, has gained lots of attention due to its newly discovered amazing and unique characteristics [18,19], such as light weight, high electrical conductivity, large surface area, excellent mechanical strength, and three-dimensional flexibility [20,21]. Many studies [20–23] showed that CNTs can significantly improve the short circuit current density (J_{sc}) and power conversion efficiency (η) of dye-sensitized solar cells (DSSCs). In our previous study [24], we concluded that QDSSCs based on 0.2 weight (wt.)% of SWCNTs/TiO_2 nanocomposite photoanode achieve 58% increase in η compared with those based on plain TiO_2 NPs photoanodes under a AM1.5 stimulated sunlight. Fang et al. [9] showed that η of DSSCs based on graphene oxide/TiO_2 photoelectrodes are remarkably higher than those of pure TiO_2. Peining et al. [25] showed that 32% enhancement in η for DSSCs based on CNTs/TiO_2 nanocomposite photoanodes.

In this study, we prepared different ratios (0.05, 0.1, 0.2, 0.5, and 1.0 wt.%) of graphene (G) in TiO_2 NPs (G/TiO_2) to formulate nanocomposite pastes for photovoltaic applications. Using SILAR technique, CdS QDs as a sensitizer were adsorbed onto G/TiO_2 nanocomposite films to form photoanodes. Graphene effect on the photovoltaic parameters (J_{sc}, open circuit voltage (V_{oc}), fill factor (*FF*), and η) of CdS QDSSCs incorporated by G/TiO_2 nanocomposite photoanodes is investigated. The electron–hole back recombination rates of the assembled QDSSCs are reported by V_{oc} decay measurements. The lifetime decay constants (τ) are also calculated.

2. Experiment

2.1. Preparation of graphene/TiO_2 nanocomposite paste

A colloidal paste of TiO_2 NPs was prepared according to our previous work [1] as follows: 3 g of commercial Degussa P25 TiO_2 nanopowders (P25) (Degussa AG, Dusseldorf, Germany) was ground in a porcelain mortar, pestle, and then mixed with 1 mL of distilled water containing acetyl acetone (10% v/v). Acetyl acetone was used as a dispersing agent because it prevents the coagulation of TiO_2 NPs and affects the porosity of the film. The paste was diluted further by the slow addition of distilled water (4 mL) under continued grinding. The addition of water controls the viscosity and final concentration of the paste. Finally, a few drops of a detergent (Triton X-100) were added, reducing the surface tension of the paste, to facilitate even spreading and reducing the formation of surface cracks.

To obtain G/TiO_2 nanocomposite pastes at different concentrations of graphene (containing 0.05, 0.1, 0.2, 0.5, and 1.0 wt.% of graphene in TiO_2 NPs as a host matrix), the method of Sacco et al. [11] was followed. Briefly, graphene powder (thickness = 0.55–3.74 nm, size = 0.5–3.0 μm, purity > 99%, purchased from Chengdu Organic Chemicals Co. Ltd.) was dissolved in ethanol and treated in an ultrasonic bath for 15 min. to form a stable colloidal dispersion. From the obtained solution, different amounts of liquid were taken out in order to obtain different concentrations of graphene in the nanocomposites. They were mixed with TiO_2 NPs paste and processed in an ultrasonic bath for 30 min., thus obtaining G/TiO_2 nanocomposite pastes at different ratios.

Using the Doctor Blade technique, each G/TiO_2 nanocomposite paste was coated on a transparent conducting glass substrate made from SnO_2: F (FTO) (purchased from Solaronix, TCO22–7, sheet resistance = 7 Ω/sq, and >80% transmittance in the visible region) and labeled from a to *f* (0, 0.05, 0.1, 0.2, 0.5, and 1.0 wt.% of G/TiO_2). Then, the films were sintered at 450 °C for 1 h. For comparison, a reference photoanode exploiting the bare TiO_2 paste without G inclusion was fabricated through the same procedure. After cooling to room temperature, CdS QDs were deposited on the G/TiO_2 nanocomposite photoanodes layer by SILAR deposition method. Two separated solutions of 0.5 M $Cd(NO_3)_2$ in ethanol and 0.5 M Na_2S in methanol were prepared. G/TiO_2 nanocomposite photoanodes were dipped into 0.5 M $Cd(NO_3)_2$ solution for 30 s and rinsed with ethanol and then, dipped into 0.5 M Na_2S for 30 s and rinsed again with methanol. The two-step dipping procedure was considered to be one cycle. This sequential coating was repeated for 6 cycles to each photoanode (a to f). After solvent evaporation, the final nanocomposite films thickness was 8 ± 1 μm. The photoanodes were then kept at room temperature. The counter electrodes were FTO substrate sheets coated with Pt.

2.2. Assembly of CdS QDSSC

The working photoanode and Pt counter electrode were assembled into a sandwich type cell using clamps. Both electrodes were sealed using a hot-melt polymer sheet (Solaronix, SX1170-25PF) that was 25 μm thick to avoid evaporation of the electrolyte. The active area of the assembled cells was 1 cm × 1 cm. Finally, an iodide electrolyte solution was prepared by dissolving 0.127 g of 0.05 M iodine (I_2) in 10 mL of water-free ethylene glycol and then adding 0.83 g of 0.5 M potassium iodide (KI). The electrolyte was inserted into the cell with a syringe, filling the space between the two electrodes.

2.3. Measurements

The absorption spectra of the working photoanodes were recorded using a UV–vis. spectrophotometer (JASCO V-670). The current density–voltage (*J–V*) characteristics were recorded with a Keithley 2400 voltage source/ammeter using Green Mountain IV-Sat 3.1 software, while the CdS QDSSCs were subjected to a solar simulator (ABET technologies, Sun 2000 Solar Simulators, USA) operating at 100 mW/cm^2 (AM1.5). The intensity of the incident solar illumination was adjusted to 1 sun condition using a Leybold certified silicon reference solar cell (Model: (57,863) Solar cell 2 V/0.3 A STE 4 /100). The photoelectric conversion efficiency η was calculated according to the following equation [26]:

$$\eta(\%) = \frac{V_{opt} \cdot I_{opt}}{P_{in}} \times 100 = \frac{V_{oc} \cdot I_{sc} \cdot FF}{P_{in}} \times 100 \quad (1)$$

where V_{opt} and I_{opt} are the optimal voltage and current respectively, *FF* is the fill factor and given as [27]:

$$FF = \frac{V_{opt} \cdot I_{opt}}{V_{oc} \cdot I_{sc}} \quad (2)$$

The photovoltage decay rates of the assembled CdS QDSSCs were measured using Tektronix 500 MHz oscilloscope. All experiments were carried out under ambient conditions.

3. Results and discussion

3.1. Characterization of CdS QDs sensitized G/TiO_2 nanocomposite photoanodes (the working photoanodes)

Fig. 1 shows the UV–vis. absorption spectra (JASCO V-670 spectrophotometer) of CdS QDs sensitized G/TiO_2 nanocomposite photoanodes for different G ratios. It is clearly seen that there is a noticeable absorption edge at 465 nm wavelength for CdS QDs sensitized G/TiO_2 nanocomposite photoanodes, which indicates the contribution from CdS QDs. The energy band gap ($E = h\ c/\lambda$) of CdS QDs corresponding to the absorption edge is equal to 2.67 eV. This blue shift with respect to bulk CdS (2.482 eV [28]) is due to the quantum confinement effect [29]. The corresponding CdS QD size can be calculated using the effective mass approximation (EMA) model [1,30]:

$$E_{g(\mathrm{Nano})}(R) = E_{g(\mathrm{bulk})} + \frac{h^2}{8R^2}\left[\frac{1}{m_e} + \frac{1}{m_h}\right] - \frac{1.8e^2}{4\pi\varepsilon\varepsilon_0 R} \tag{3}$$

where m_e (0.21 m_0) and m_h (0.64 m_0) [28] are the effective masses of the electron and hole, respectively, m_0 is the electron mass, $E_{g(\mathrm{bulk})}$ (2.482 eV) is the bulk crystal band gap, R is the average radius of the nanocrystal, $E_{g(\mathrm{Nano})}$ is the QD band gap value, h is Planck's constant and ε (5.7) [28] is the relative permittivity. The calculated average size of CdS QDs based on Eq. (3) is 5.12 nm.

The UV–vis. absorption spectra of plain TiO_2 NPs photoanode, 0.2 wt.% G/TiO_2 nanocomposite photoanode, CdS QDs sensitized plain TiO_2 NPs photoanode, and CdS QDs sensitized 0.2 wt.% G/TiO_2 nanocomposite photoanode are shown in Fig. 2. It is clearly observed that the absorption of CdS QDs sensitized G/TiO_2 nanocomposite photoanode is higher than that of CdS QDs sensitized plain TiO_2 NPs photoanode, indicating that additional amount of CdS QDs have been deposited onto the TiO_2 NPs incorporated with G films. The increase of CdS QDs loading amount is due to the increase of specific surface area and the porosity when G is introduced into TiO_2 NPs films [9,31].

3.2. Photovoltaic performance of CdS QDSSCs using G/TiO_2 nanocomposite photoanode

The photocurrent density–voltage (J–V) characteristics were used to investigate the effect of G ratio in TiO_2 photoanodes on the photovoltaic performance of CdS QDSSCs. Fig. 3 shows the J–V characteristics curves of CdS QDSSCs measured under a simulated sunlight with an intensity of 100 mW/cm^2 (AM 1.5G). The photovoltaic characteristics parameters (V_{oc}, J_{sc}, FF, and η) for CdS QDSSCs are given in Table 1. It is clearly seen that as G ratio increases up to 0.2 wt.%, the values of J_{sc}, V_{oc}, and η increase, peaking at 1.83 mA/cm^2, 0.67 V, and 0.37% respectively for photoanode (c). These values decrease for photoanode (e) corresponding for 0.5 wt.% G/TiO_2 (1.54 mA/cm^2, 0.65 V, and 0.31%) and (f) for 1.0 wt.%

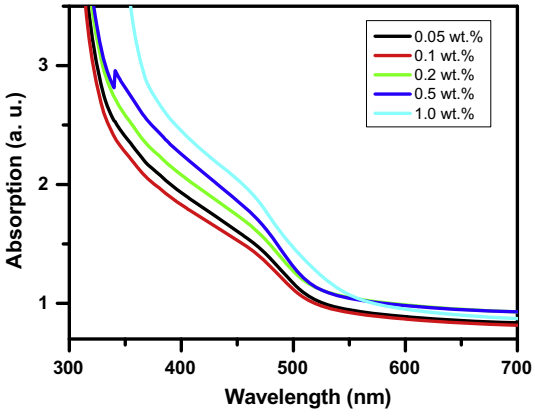

Fig. 1. UV–vis. absorption spectra of CdS QDs sensitized G/TiO_2 nanocomposite photoanodes for different G ratios.

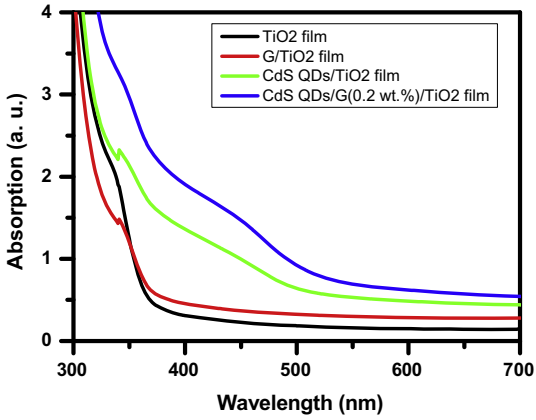

Fig. 2. UV–vis. absorption spectra of plain TiO_2 photoanode, G/TiO_2 nanocomposite photoanode, CdS QDs/TiO_2 NPs photoanode, and CdS QDs/G (0.2 wt.%)/TiO_2 nanocomposite photoanode.

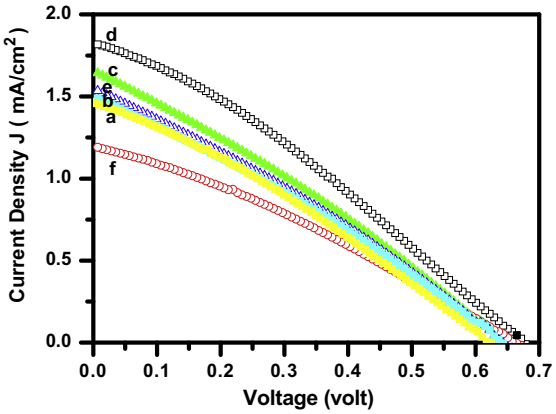

Fig. 3. *J–V* characteristics curves of CdS QDSSCs using G/TiO_2 nanocomposite photoanodes for different G ratios: (a) 0, (b) 0.05, (c) 0.1, (d) 0.2, (e) 0.5, and (f) 1.0 wt.%.

Table 1
J–V characteristics parameters of CdS QDSSCs using G and TiO_2 photoanodes for different G ratios.

G ratio (wt.%)	V_{oc} (Volt) ± 0.01	J_{sc} (mA/cm^2) ± 0.01	*FF*	η (±0.01)%
0	0.61	1.45	0.31	0.28
0.05	0.65	1.50	0.34	0.30
0.1	0.66	1.64	0.33	0.32
0.2	0.67	1.83	0.32	0.37
0.5	0.65	1.54	0.34	0.31
1.0	0.64	1.21	0.33	0.22

G/TiO_2 (1.21 mA/cm^2, 0.64 V, and 0.22%). This result could be explained in terms of G ratio: as G/TiO_2 ratio increases up to 0.2 wt.%, an additional amounts of CdS QDs are loaded because of high roughness and porous surface of G/TiO_2 nanocomposite [31], which lead to the improvement in the absorption of the nanocomposite films as shown in Fig. 1. Moreover, G sheets have excellent electrical conductivity

and could therefore act as bridges to accelerate electron transfer from TiO_2 to the FTO electrode, reducing the possibility of electron–hole recombination rates. Besides, graphene with a two-dimensional structure can capture more TiO_2 nanoparticles which provide electronic-transport tunnel and shorten the electronic transmission way [32]. On the other hand, when G/TiO_2 ratio was further increased from 0.2 to 1.0 wt.%, J_{sc} of CdS QDSSC started to decrease from 1.83 mA/cm^2 to 1.21 mA/cm^2 and η decreased from 0.37% to 0.22%. This is due to many reasons: (a) the excessive of G can act as a kind of recombination center instead of providing an electron pathway, and a short circuit will happen easily, then reduces η [26]. (b) The extra amount of G causes light harvesting competition between CdS QDs and G, also QDs coverage on TiO_2 surface will reduce due to TiO_2 is surrounded by more graphene [11,18]. (c) High concentration of G in the photoanode makes it less optically transparent and hence the light harvesting of CdS QDs will be decreased [25]. Our results are in good agreement with others [25,26]. Peining et al. [25] fabricated a DSSCs using TiO_2 coated CNTs (TiO_2-CNTs) photoanodes with different CNTs concentrations (0–0.3 wt.%). In their work, they concluded that the photovoltaic parameters increased with increases in CNT concentrations, reach a maximum and then decreased. The optimum concentration of CNTs in the TiO_2 matrix for best performance in DSSCs is found to be 0.2 wt.%, which shows a 32% enhancement in the energy conversion efficiency. Kim et al. [33] investigated the effect of graphene concentration (varies from 0 to 1.0 wt.% in G/TiO_2 photoanodes) on η of DSSCs. They found that the optimal concentration was 0.3 wt.%, which decreased the recombination rate, where at higher concentrations than 0.3 wt.%, η decreased owing to higher absorption of light by graphene present on the surface, thus reducing the generation of electron–hole pairs.

Fig. 4 shows schematic energy diagram of CdS QDSSC using G/TiO_2 photoanode. The stepwise energy levels of CdS QDs, TiO_2, G, and FTO are beneficial for electrons to transport from the conduction band of CdS QDs to FTO substrate. A suitable ratio of G bridges behaves as an electron transfer channel, that can transport the generated electrons quickly and without any obstruction, since G energy level is between the conduction band (CB) of TiO_2 and FTO, and hence the adverse reactions recombination and back reaction are suppressed.

The electron–hole recombination rates of CdS QDSSCs were determined by photovoltage-decay measurements. Fig. 5(a) shows V_{oc} decay rates of CdS QDSSCs based on: plain TiO_2 NPs photoanode, 0.2 wt.% ratio of G/TiO_2, and 0.5 wt.% ratio of G/TiO_2 nanocomposite photoanodes using a 500 MHz oscilloscope (Tektronix). It is clearly seen that V_{oc} decay rate of CdS QDSSCs based on G/TiO_2 nanocomposite photoanode is slower than that using plain TiO_2 NPs photoanode. Moreover, V_{oc} decay rate of QDSSCs based on 0.2 wt.% ratio of G/TiO_2 nanocomposite photoanodes is much slower than that based on 0.5 wt.% ratio of G/TiO_2 photoanodes. This novel verification indicates that electron back recombination rates decrease significantly with the existence of G in the nanocomposite photoanodes. Thereby, appropriate ratio of G in TiO_2 enhances the photovoltaic performance of CdS QDSSCs. The electron lifetime constants (τ) as a function of the decaying V_{oc} were calculated from Eq. (4) [34,35]:

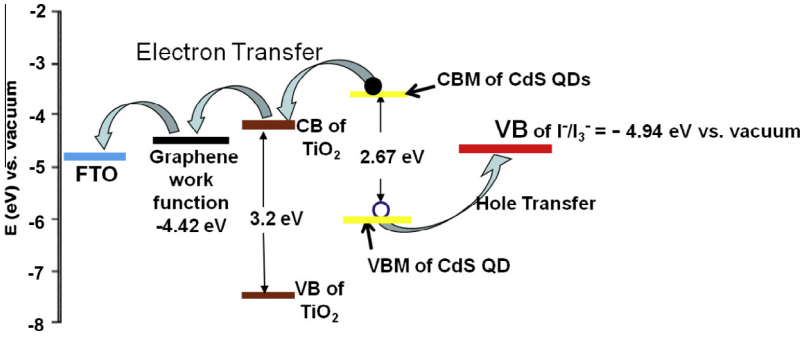

Fig. 4. Schematic energy diagram of CdS QDSSC using G/TiO_2 photoanode. The Fermi level of TiO_2, graphene and redox (I^-/I_3^-) are set at −4.21 [33], −4.42 [33], and −4.94 eV [16] respectively.

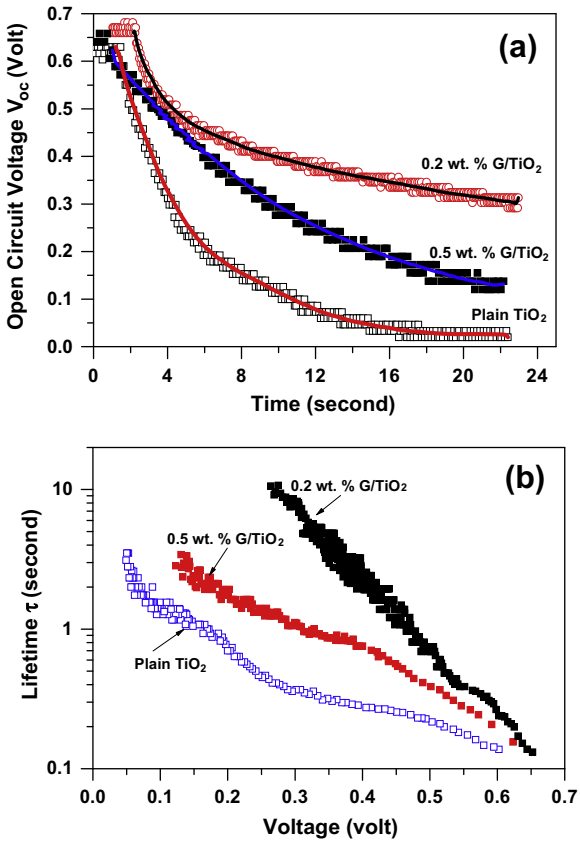

Fig. 5. (a) The open circuit voltage (V_{oc}) decay rate of CdS QDSSCs based on: plain TiO_2 NPs photoanode, 0.2 wt.% ratio of G/TiO_2, and 0.5 wt.% ratio of G/TiO_2 nanocomposite photoanodes, and (b) the electron lifetime τ as a function of voltage from Eq. (4).

$$\tau = -\frac{k_B}{e}\left(\frac{dV_{oc}}{dt}\right)^{-1} \tag{4}$$

The lifetime constants (τ) of CdS QDSSCs based on: plain TiO_2 NPs photoanode, 0.2 wt.% ratio of G/TiO_2, and 0.5 wt.% ratio of G/TiO_2 nanocomposite photoanodes are shown in Fig. 5(b). It is clearly seen that τ for CdS QDSSCs based on G/TiO_2 nanocomposite photoanode is larger than that based on plain TiO_2 NPs photoanode. This novel result verifies that appropriate ratio of G in TiO_2 acts the role of a blocking layer to suppress the back electron–hole recombination in QDSSCs and thus enhancing the energy conversion efficiency η.

4. Conclusion

We have synthesized nanocomposite pastes of different graphene/titania (G/ TiO_2) ratios (0, 0.1, 0.2, 0.5, and 1.0 wt.%) to fabricate photoanodes for CdS quantum dots sensitized solar cells (QDSSCs). CdS QDs as a sensitizer were deposited onto G/TiO_2 nanocomposite films by successive ionic layer adsorption and reaction (SILAR) technique for six cycles. The optimal G/TiO_2 ratio was 0.2 wt.% for CdS QDSSCs. A significant enhancement (~32%) in the energy conversion efficiency (η) was achieved in CdS QDSSCs based on 0.2 wt.% ratio of G/TiO_2 nanocomposite as compared to others' based on plain TiO_2 NPs under a AM1.5 simulated sunlight. The open circuit voltage (V_{oc}) decay rate of CdS QDSSCs

based on 0.2 wt.% ratio of G/TiO_2 nanocomposite photoanodes is much slower than those using plain TiO_2 NPs photoanodes. This novel evidence indicates that electron–hole back recombination rates decrease significantly with CdS QDSSCs based on 0.2 wt.% ratio of G/TiO_2 nanocomposite photoanodes. The lifetime constants (τ) for CdS QDSSCs based on 0.2 wt.% ratio of G/TiO_2 nanocomposite photoanodes is much larger than those based on bare TiO_2 NPs photoanodes.

Acknowledgements

I wish to thank Taif University for the Grant research No. (1/435/3524). The Quantum Optics group at Taif University is also thanked for their assistance during this work.

References

[1] A. Badawi, N. Al-Hosiny, S. Abdallah, S. Negm, H. Talaat, Tuning photocurrent response through size control of CdTe quantum dots sensitized solar cells, Sol. Energy 88 (2013) 137–143.
[2] A. Tubtimtae, M.-W. Lee, G.-J. Wang, Ag_2Se quantum-dot sensitized solar cells for full solar spectrum light harvesting, J. Power Sources 196 (2011) 6603–6608.
[3] A. Salant, M. Shalom, I. Hod, A. Faust, A. Zaban, U. Banin, Quantum dot sensitized solar cells with improved efficiency prepared using electrophoretic deposition, ACS Nano 4 (2010) 5962–5968.
[4] A. Kongkanand, K. Tvrdy, K. Takechi, M. Kuno, P.V. Kamat, Quantum dot solar cells. Tuning photoresponse through size and shape control of CdSe–TiO_2 architecture, J. Am. Chem. Soc. 130 (2008) 4007–4015.
[5] B. Li, T. Liu, Y. Wang, Z. Wang, ZnO/graphene-oxide nanocomposite with remarkably enhanced visible-light-driven photocatalytic performance, J. Colloid Interface Sci. 377 (2012) 114–121.
[6] K. Tvrdy, P.V. Kamat, Substrate driven photochemistry of CdSe quantum dot films: charge injection and irreversible transformations on oxide surfaces, J. Phys. Chem. A 113 (2009) 3765–3772.
[7] A. Badawi, N. Al-Hosiny, S. Abdallah, H. Talaat, Tuning photocurrent response through size control of CdSe quantum dots sensitized solar cells, Mater. Sci.-Poland 31 (2013) 6–13.
[8] C.Y. Neo, J. Ouyang, Graphene oxide as auxiliary binder for TiO_2 nanoparticle coating to more effectively fabricate dye-sensitized solar cells, J. Power Sources 222 (2013) 161–168.
[9] X. Fang, M. Li, K. Guo, Y. Zhu, Z. Hu, X. Liu, B. Chen, X. Zhao, Improved properties of dye-sensitized solar cells by incorporation of graphene into the photoelectrodes, Electrochim. Acta 65 (2012) 174–178.
[10] N. Al-Hosiny, S. Abdallah, A. Badawi, K. Easawi, H. Talaat, The photovoltaic performance of alloyed $CdTe_xS_{1-x}$ quantum dots sensitized solar cells, Mater. Sci. Semicond. Process. 26 (2014) 238–243.
[11] A. Sacco, S. Porro, A. Lamberti, M. Gerosa, M. Castellino, A. Chiodoni, S. Bianco, Investigation of transport and recombination properties in graphene/titanium dioxide nanocomposite for dye-sensitized solar cell photoanodes, Electrochim. Acta 131 (2014) 154–159.
[12] S. Abdallah, N. Al-Hosiny, A. Badawi, Photoacoustic study of CdS QDs for application in quantum-dot-sensitized solar cells, J. Nanomater. 2012 (2012) 6.
[13] F. Zhao, G. Tang, J. Zhang, Y. Lin, Improved performance of CdSe quantum dot-sensitized TiO_2 thin film by surface treatment with $TiCl_4$, Electrochim. Acta 62 (2012) 396–401.
[14] S. Kitada, E. Kikuchi, A. Ohnob, S. Aramakib, S. Maenosono, Effect of diamine treatment on the conversion efficiency of PbSe colloidal quantum dot solar cells, Solid State Commun. 149 (2009) 1853–1855.
[15] Y. Liu, J. Wang, Co-sensitization of TiO_2 by PbS quantum dots and dye N719 in dye-sensitized solar cells, Thin Solid Films 518 (2010) e54–e56.
[16] P. Yu, K. Zhu, A.G. Norman, S. Ferrere, A.J. Frank, A.J. Nozik, Nanocrystalline TiO_2 solar cells sensitized with InAs quantum dots, J. Phys. Chem. B 110 (2006) 25451–25454.
[17] Y. Hu, B. Wang, J. Zhang, T. Wang, R. Liu, J. Zhang, X. Wang, H. Wang, Synthesis and photoelectrochemical response of CdS quantum dot-sensitized TiO_2 nanorod array photoelectrodes, Nanoscale Res. Lett. 8 (2013) 222.
[18] N. Yang, J. Zhai, D. Wang, Y. Chen, L. Jiang, Two-dimensional graphene bridges enhanced photoinduced charge transport in dye-sensitized solar cells, ACS Nano 4 (2010) 887–894.
[19] A.-Y. Kim, J. Kim, M.Y. Kim, S.W. Ha, N.T.T. Tien, M. Kang, Photovoltaic efficiencies on dye-sensitized solar cells assembled with graphene-linked TiO_2 anode films, Bull. Korean Chem. Soc. 33 (2012) 3355–3360.
[20] J. Yan, M.J. Uddin, T.J. Dickens, O.I. Okoli, Carbon nanotubes (CNTs) enrich the solar cells, Sol. Energy 96 (2013) 239–252.
[21] H. Chang, T.-J. Hsieh, T.-L. Chen, K.-D. Huang, C.-S. Jwo, S.-H. Chien, Dye-sensitized solar cells made with TiO_2-coated multi-wall carbon nanotubes and natural dyes extracted from ipomoea, Mater. Trans. 50 (2009) 2879–2884.
[22] J.Y. Ahn, J.H. Kim, K.J. Moon, J.H. Kim, C.S. Lee, M.Y. Kim, J.W. Kang, S.H. Kim, Incorporation of multiwalled carbon nanotubes into TiO_2 nanowires for enhancing photovoltaic performance of dye-sensitized solar cells via highly efficient electron transfer, Sol. Energy 92 (2013) 41–46.
[23] G. Khurana, S. Sahoo, S.K. Barik, R.S. Katiyar, Improved photovoltaic performance of dye sensitized solar cell using ZnO-graphene nano-composites, J. Alloys Compd. 578 (2013) 257–260.
[24] A. Badawi, N. Al-Hosiny, S. Abdallah, A. Merazga, H. Talaat, Single wall carbon nanotube/titania nanocomposite photoanodes enhance the photovoltaic performance of cadmium selenide quantum dot-sensitized solar cells, Mater. Sci. Semicond. Process. 26 (2014) 162–168.
[25] Z. Peining, A.S. Nair, Y. Shengyuan, P. Shengjie, N.K. Elumalai, S. Ramakrishna, Rice grain-shaped TiO_2-CNT composite—a functional material with a novel morphology for dye-sensitized solar cells, J. Photochem. Photobiol., A 231 (2012) 9–18.

[26] J. Yu, J. Fan, B. Cheng, Dye-sensitized solar cells based on anatase TiO_2 hollow spheres/carbon nanotube composite films, J. Power Sources 196 (2011) 7891–7898.
[27] S. Emin, S.P. Singh, L. Han, N. Satoh, A. Islam, Colloidal quantum dot solar cells, Sol. Energy 85 (2011) 1264–1282.
[28] O. Madelung, Semiconductors: Data Handbook, third ed., Springer-Verlag, Berlin, 2004.
[29] N. Al-Hosiny, A. Badawi, M.A.A. Moussa, R. El-Agmy, S. Abdallah, Characterization of optical and thermal properties of CdSe quantum dots using photoacoustic technique, Int. J. Nanoparticles 5 (2012) 258–266.
[30] L. Brus, Electronic wave functions in semiconductor clusters: experiment and theory, J. Phys. Chem. 90 (1986) 2555–2560.
[31] E.S. Lee, K.M. Lee, S.I. Yoon, Y.G. Ko, D.H. Shin, Influence of CNT incorporation on the photovoltaic behavior of TiO_2 films formed by high-voltage electrophoretic deposition, Curr. Appl. Phys. 13 (Suppl 2) (2013) S26–S29.
[32] L. Chen, L. Tuo, J. Rao, X. Zhou, TiO_2 doped with different ratios of graphene and optimized application in CdS/CdSe quantum dot-sensitized solar cells, Mater. Lett. 124 (2014) 161–164.
[33] D.-Y. Kim, B.N. Joshi, J.-J. Park, J.-G. Lee, Y.-H. Cha, T.-Y. Seong, S. In Noh, H.-J. Ahn, S.S. Al-Deyabe, S.S. Yoon, Graphene–titania films by supersonic kinetic spraying for enhanced performance of dye-sensitized solar cells, Ceram. Int. 40 (2014) 11089–11097.
[34] F. Al-Juaid, A. Merazga, A. Al-Baradi, F. Abdel-wahab, Effect of sol–gel ZnO spin-coating on the performance of TiO_2-based dye-sensitized solar cell, Solid-State Electron. 87 (2013) 98–103.
[35] J. Kim, H. Choi, C. Nahm, J. Moon, C. Kim, S. Nam, D.-R. Jung, B. Park, The effect of a blocking layer on the photovoltaic performance in CdS quantum-dot-sensitized solar cells, J. Power Sources 196 (2011) 10526–10531.